Surface structure of Rh(001) and $p(1\times1)$ H on Rh(001): An unresolved discrepancy between experiment and theory

G. Teeter, D. Hinson, and J. L. Erskine
Department of Physics, The University of Texas at Austin, Austin, Texas 78712

C. B. Duke and A. Paton
Xerox Wilson Center, Webster, New York 14580

(Received 11 July 1997; revised manuscript received 19 September 1997)

Low-energy-electron diffraction intensity measurements and analysis are used to obtain multilayer surface relaxation of clean and hydrogen-saturated Rh(001). Results averaged over three data sets show the first interlayer spacing of clean Rh(001) to be expanded ($+1.0\%\pm0.6\%$) relative to the bulk spacing (1.902 Å) and the second interlayer spacing to be contracted ($-0.7\%\pm0.5\%$). Chemisorbed hydrogen atoms are found to reside at fourfold hollow sites 0.88 ± 0.05 Å above the Rh(001) surface, and to modify significantly the first ($+4.1\pm1.0\%$) and second ($-2.2\%\pm1.0\%$) interlayer spacing relative to bulk values. These results confirm the existence of systematic differences between calculated and measured multilayer relaxation of Rh(001). [S0163-1829(98)04407-5]

I. INTRODUCTION

Systematic discrepancies between first-principles calculations[1–5] and experimental determinations[6–9] of the surface relaxation of Rh(001), and more generally of selected reactive transition metals,[2] have been a subject of recent interest. The magnitude of discrepancies generally exceeds the accepted accuracy of both the experiments and the theoretical calculations. This situation, therefore, appears to present a dilemma worthy of further investigation. Central issues associated with these discrepancies, and reference to the corresponding experimental and theoretical work on Ti(0001), Zr(0001), Ru(0001), Mo(110), W(110), and Rh(001) have recently been presented by Feibelman.[2] Specifically, modern *ab initio* calculations systematically predict top-layer relaxations of these surfaces that are a factor of 2–5 larger than the experimentally determined values.[10]

Several phenomenological models[2,11] that attempt to account for trends in surface relaxation have been proposed. The charge smoothing model[12–14] based on ideas proposed by Smoluchowski[12] and Finnis and Heine[13] (FH), appears to explain why most outer surface layers of metals relax inward. The FH model predicts larger contraction on more open surfaces, and can even account for small outward relaxations on close-packed surfaces. The bond order model[14] also accounts for the generally observed inward surface relaxation and predicts larger contractions for more open crystal faces. The bond order model, which is a ''chemical'' model based on promotion-hybridization arguments, can yield large relaxations ($>2\%$) even for close-packed surfaces while also accounting for the outward relaxation of Be(0001).[2] Based on the above models, an outward relaxation of Rh(001), or even an ideal ''bulk termination'' at the surface, is difficult to explain. An accurate surface structure determination for Rh(001) may help clarify or at least more precisely define the surface relaxation dilemma, and may also help refine our qualitative understanding of surface relaxation based on these phenomenological models.

To obtain a better appreciation of this issue and recent attempts to resolve it, we focus our attention in this paper on one of the metal surfaces in question: Rh(001). Table I contains a summary of the first- and second-layer surface relaxations for Rh(001) determined by prior low-energy-electron diffraction (LEED) experiments,[6–8] photoelectron diffraction experiments,[9] and by recent *ab initio* calculations.[1–6] Early calculations[1] based on a linear-augmented-plane-wave (LAPW) method predicted a significant first-layer contraction ($\Delta d_{12}/d_0=-5.1\%$, where $d_0=1.902$ Å is the bulk lattice spacing) in agreement with

TABLE I. First- and second-layer surface relaxation of Rh(001) in terms of percent of bulk interlayer spacing, $d_0=1.902$ Å.

Experiment	$\Delta d_{12}/d_0(\%)$	$\Delta d_{23}/d_0\%$
Watson *et al.*[a]	-1.0 ± 0.9	
Oed *et al.*[b]	$+0.5\pm1.0$	$+0.0\pm1.5$
Begley *et al.*[c]	-1.16 ± 1.6	$+0.0\pm1.6$
Prince *et al.*[d]	-1.14 ± 3.6	
Present work	$+1.0\pm0.6$	-0.7 ± 0.5
Theory		
Feibelman and Hamann[e]	-5.1	-0.5
Morrison, Bylander, and Kleinman[f,g]	-1.52	$+0.98$
Cho and Scheffler[h] (GGA)	-2.8	-0.1
(GGA at 300 K)	-1.4	
(LDA)	-3.0	-0.2
Eichler *et al.*[i]	-3.8 ± 0.1	$+0.7$

[a]Reference 6.
[b]Reference 7.
[c]Reference 8.
[d]Reference 9.
[e]Reference 1.
[f]Reference 3.
[g]Surface predicted to be ferromagnetic.
[h]Reference 5.
[i]Reference 4.

what was generally expected for a transition metal surface. The existing LEED results[6,7] ($\Delta d_{12}/d_0 = +0.5 \pm 1.0\%$) suggested a small outward relaxation. Feibelman and Hamann[1] proposed a possible explanation that could account for the large discrepancy: contamination of the surface by residual hydrogen. A second possible explanation based on ''magnetic pressure'' resulting from (unconfirmed) surface magnetism of Rh(001) was proposed by Morrison, Bylander, and Kleinman.[3]

Subsequent calculations[4–5] and experiments[15] have addressed the surface magnetism issue. Ferromagnetism is favored when the energy gained by removing spin degeneracy is greater than the gain in kinetic energy as more electrons fill the majority spin band. Since the increase in kinetic energy is less when the interatomic separation is greater, larger atomic volumes favor ferromagnetism. These considerations have led to exploration of the possibility of two-dimensional (2D) magnetism in $4d$ transition metals (including Rh). Bulk Rh nearly fulfills the Stoner criterion for ferromagnetism, so that the expected narrower density of d states at the surface could stabilize a surface magnetic ground state. Recent local-density-approximation (LDA) calculations for Rh(001) either predict surface ferromagnetism[3] with a corresponding increase in d_{12} (see Table I), or predict that the ferromagnetic state of surface atoms is essentially degenerate with the nonmagnetic[4,5] state. The more recent calculations predict smaller d_{12} contractions than prior calculations, but neither approaches the unrelaxed or slightly expanded value determined by LEED. Spin-polarized photoemission experiments[15] carried out on clean Rh(001) detect the existence of a spin-polarized surface resonance at the M point in the surface Brillouin zone at room temperature, suggesting that the surface is weakly ferromagnetic. Ferromagnetism of the Rh(001) surface cannot, however, be considered as having been confirmed.

The most recent LEED study of Rh(001) by Begley *et al.*[8] suggests that the surface is relaxed by $-1.2\% \pm 1.6\%$. This result is compatible with the earlier LEED studies (based on the error bars assigned to the various structure determinations) and is in better agreement with the theoretical work. None of the LEED analyses of Rh(001) directly addresses the hydrogen issue, although Begley *et al.*[8] present plausible arguments based on other experiments that suggest surface hydrogen is not a significant factor in their results. The Rh(001) surface has also recently been studied by surface core-level shift (SCLS) photoelectron diffraction.[9] Preliminary evaluation of the data yields a first-layer surface relaxation $\Delta d_{12}/d_0$ of $-1.4\% \pm 3.6\%$ in better agreement with theoretical results and consistent with the experimental result of Begley *et al.*[8] Surface core-level shifts are sensitive to surface contamination, and the SCLS technique therefore permits monitoring hydrogen contamination during the acquisition of structure sensitive data. The SCLS data set used to obtain the reported value of $\Delta d_{12}/d_0$ is rather limited (~ 150 eV kinetic energy range), and the error bars are correspondingly large.

In this paper we present the results of a LEED study of Rh(001) with special attention directed to the issues just outlined. Specifically, our objectives in undertaking the LEED study of Rh(001) were to deal definitively with the issue of hydrogen contamination and to refine the LEED structure analysis sufficiently to be able to differentiate between an expanded[6,7] and contracted[8,9] surface layer. We also determine the surface structure of the H saturated Rh(001) surface including the Rh-H interplanar distance. We proceed by indicating our sample preparation and data acquisition procedures in Sec. II. In Sec. III we describe our model calculations of the LEED intensities. The results of our structure analysis are presented in Sec. IV and discussed in Sec. V.

II. EXPERIMENTAL PROCEDURES

Our experiments were carried out using a UHV instrument that incorporates Varian four-grid LEED optics, a Physical Electronics double pass Auger analyzer, and a Leybold ELS-22 electron energy-loss spectrometer (EELS). The instrument base pressure is typically 5×10^{-11} torr; essentially all H and CO when monitored by a quadrupole mass spectrometer. LEED intensity data were obtained using a SIT camera interfaced to an IBM PC via frame grabbing instrumentation. The linearity and dynamic range (8 bit) of the camera was carefully evaluated, and measured intensities were normalized to the electron gun current which was calibrated by measuring the sample current when biased at $+90$ V. The Rh(001) surface was cleaned by repeated cycles of high-temperature annealing in O_2 followed by flashing and characterized by Auger analysis (C and O) and EELS (H).

A series of EELS experiments, conducted at base pressures ($5 \times 10^{-11} - 2 \times 10^{-10}$ torr) and at hydrogen dosing pressures ($10^{-9} - 10^{-7}$ torr) with the sample held at temperatures ranging from 100–350 K, established the H uptake characteristics of Rh(001) necessary to evaluate the H coverage during LEED data acquisition under the various conditions used in our experiments. Our experimental EELS results for H adsorption on Rh(001) are in good agreement with results reported by Richter *et al.*[16] Specifically, we observed coverage-dependent shifts in vibrational loss frequencies that occur until saturation coverage is achieved. The H_2 dissociative sticking coefficient is high (essentially unity) at 100 K, and the H saturated surface yields a sharp $p(1 \times 1)$ LEED pattern and high specular elastic peak EELS intensity consistent with a well-ordered adlayer. Detailed analysis of the vibrational losses of saturated H on Rh(001) by Richter *et al.*[16] and the single symmetric thermal desorption peak observed for the H-Rh(001) system are consistent with a model in which H atoms reside at the surface in fourfold hollow sites. No evidence of subsurface hydrogen or of surface site occupation by H other than the fourfold hollow site is evident from the EELS experiments. Our dynamical LEED analysis of the $p(1 \times 1)$ H saturated Rh(001) surface, described later, is also consistent with surface H atoms in fourfold hollow sites.

In the upper panel of Fig. 1 we display an Auger spectrum of a clean Rh(001) surface showing the absence of any significant O or C contamination. The integrated hydrogen EELS loss peak intensities as a function of time for two sample temperatures at typical base pressures are shown in the lower panel of Fig. 1. From our hydrogen adsorption studies we conclude that at 100 K, 0.1 ML of H forms on clean Rh(001) at a base pressure of 1×10^{-10} torr in about 5 min, but that at temperatures near 300 K the Rh(001) surface

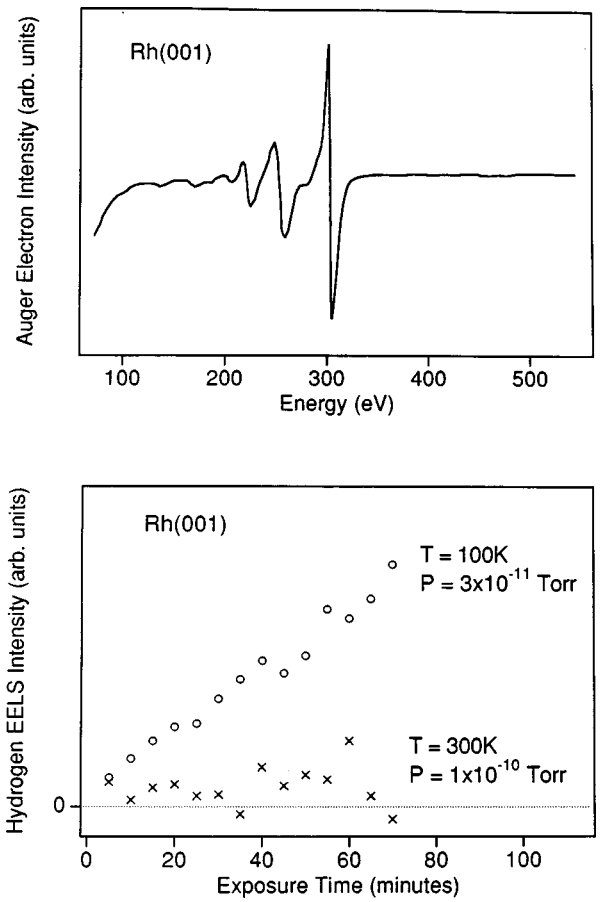

FIG. 1. Upper panel: Auger spectrum of clean Rh(001). Lower panel: measured hydrogen uptake by Rh(001) at two different temperatures.

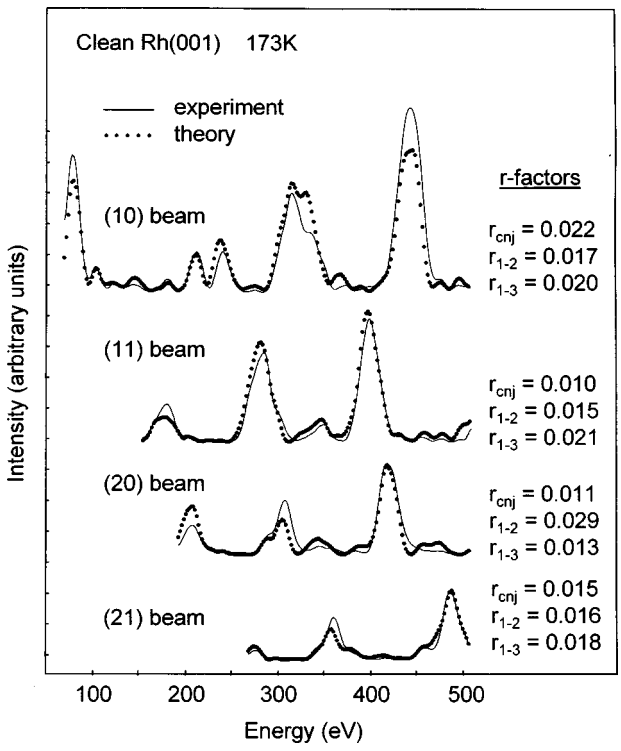

FIG. 2. Measured and calculated LEED, intensity profiles from the Van Hove/Tong codes for Rh(001). Three sets of Zanazzi-Jona r factors are indicated for each beam that compare various *experimental* spectra. They represent averages for the conjugate beams within each set (cnj) and between independent averaged data sets (set 1-2 and set 1-3 comparisons). The r factors characterizing theory/experiment comparisons are presented in Table II (Van Hove/Tong, Zanazzi-Jona, and Pendry r factors) and in Table III [r_2' and x-ray (Ref. 26) r factors].

remains essentially free of H contamination during the time required to collect a LEED data set ($\sim$60 min). The low-temperature measurements of surface H contamination rates are consistent with our calculations of H_2 impingement rates and a unity sticking coefficient at 1×10^{-10} torr.

Numerous LEED data sets were collected from the Rh(001) surface. After data reduction (frame processing to subtract background intensity) and preliminary analysis (conjugate beam comparisons, and general assessment of the quality of the data) five data sets were selected for intensity analysis: three sets for the clean surface (two at 300 K and one at 173 K) and two sets for the $p(1\times1)$ hydrogen saturated surface at 100 K. In Fig. 2 we show a complete set of conjugate beam-averaged LEED data for clean Rh(001) at 173 K and their comparison with calculated intensities that are discussed later. The r factors indicated in Fig. 2 compare *experimental* data and characterize the close similarity of conjugate beam data within each beam-averaged data set, as well as the variation of averaged beam data sets of the three distinct experimental measurements. The r factors characterizing theory-experiment comparisons are presented in Table II.

III. MODEL CALCULATIONS

Surface structure evaluations were carried out by calculating LEED intensities using the Van Hove/Tong layer-doubling code[17] and independently using the Xerox matrix-inversion code.[18,19] This procedure establishes the compatibility of two entirely independent analysis methodologies. The fact that two different multiple-scattering codes were used to generate the LEED intensity spectra is incidental: the two codes yield essentially identical results when properly normalized.

Convergence tests were conducted with the Van Hove/Tong code to show that 185 beams were more than adequate to characterize the scattered electron intensity over the 50–500 eV energy range covered by experimental data. An analogous test with the Xerox codes revealed that a complete matrix-inversion analysis of a six-layer slab accurately described results obtained using thicker slabs. Detailed comparisons of the results of both sets of codes revealed that the absolute normalizations of the Xerox and Van Hove/Tong codes are not identical. A least-squares comparison analysis was used to determine that their outputs differ by a normalization constant of $k/4$ with k being the wave number of the electron inside the medium. Structure analyses were performed using either the Van Hove/Tong codes or the intensities predicted by the Xerox codes multiplied by this factor so that the intensities calculated using either code set are essentially identical.

Electron scattering by surface atoms is described using eight energy-dependent phase shifts. Each atomic scattering

TABLE II. First (d_{12}) and second (d_{23}) interlayer spacing of Rh(001) determined by LEED structure analysis ($\Delta d_{ij}/d_{\text{Bulk}}\%$) using the Van Hove/Tong codes. RT1: room temperature data set 1; LT3: low temperature data set 3.

Data set	R factor	d_{12} (Å)	d_{23} (Å)	$d_{\text{Rh-H}}$ (Å)
RT1	$r_{\text{VHT}}=0.30$	1.91	1.89	
	$r_{\text{ZJ}}=0.11$	1.90	1.90	
	$r_{\text{P}}=0.34$	1.92	1.88	
RT2	$r_{\text{VHT}}=0.30$	1.92	1.90	
	$r_{\text{ZJ}}=0.08$	1.90	1.91	
	$r_{\text{P}}=0.35$	1.95	1.88	
LT3	$r_{\text{VHT}}=0.25$	1.92	1.88	
	$r_{\text{ZJ}}=0.07$	1.91	1.89	
	$r_{\text{P}}=0.29$	1.92	1.88	
Clean surface	Average	1.92 ± 0.01	1.89 ± 0.01	
	%	$(+0.95\pm0.5\%)$	$(-0.63\pm0.5\%)$	
LT4	$r_{\text{VHT}}=0.35$	1.96	1.86	0.88
	$r_{\text{ZJ}}=0.12$	1.95	1.86	0.90
	$r_{\text{P}}=0.37$	1.98	1.87	0.86
LT5	$r_{\text{VHT}}=0.37$	1.97	1.86	0.87
	$r_{\text{ZJ}}=0.12$	1.97	1.86	0.90
	$r_{\text{P}}=0.34$	2.01	1.85	0.88
Hydrogen surface	Average	1.98 ± 0.02	1.86 ± 0.01	0.88 ± 0.03
	%	$(+4.10\pm1.1\%)$	$(-2.21\pm0.5\%)$	

center is represented as a neutral atom whose potential is computed using a nonrelativistic self-consistent Hartree-Fock-Slater muffin-tin model.[20–22] A nonrelativistic potential was used because a prior detailed analysis of W(100) (a material having higher Z than Rh) revealed that a better description of the LEED intensities was obtained using nonrelativistic potentials in nonrelativistic scattering calculations compared to the use of relativistic potentials to generate nonrelativistic phase shifts. Also, prior LEED analysis of surfaces containing fourth row materials (i.e., InSb, CdTe) based on nonrelativistic phase shifts have yielded satisfactory results. The resulting effective-scattering potential is inserted into the radial Schrödinger equation, which is integrated to yield the scattered wave phase shifts. These are shown in Fig. 3. Comparison of phase shifts constructed from a relativistic Rh atomic potential with those from the nonrelativistic potential revealed negligible differences over the energy range (50–500 eV) covered by the analysis. Hydrogen atom phase shifts were calculated based on a simple cubic H atom lattice to define a muffin-tin potential. The lattice constant $2r_{\text{H}}=1.34$ Å was obtained from the calculated[23] height of H above Rh(001) in fourfold hollow sites.

Thermal vibrations of the atoms are incorporated into the analysis via an imaginary part of the phase shifts calculated as described by Duke *et al.*[24] The vibrations of both surface and bulk Rh atoms are described using a Debye temperature of 480 K.[25]

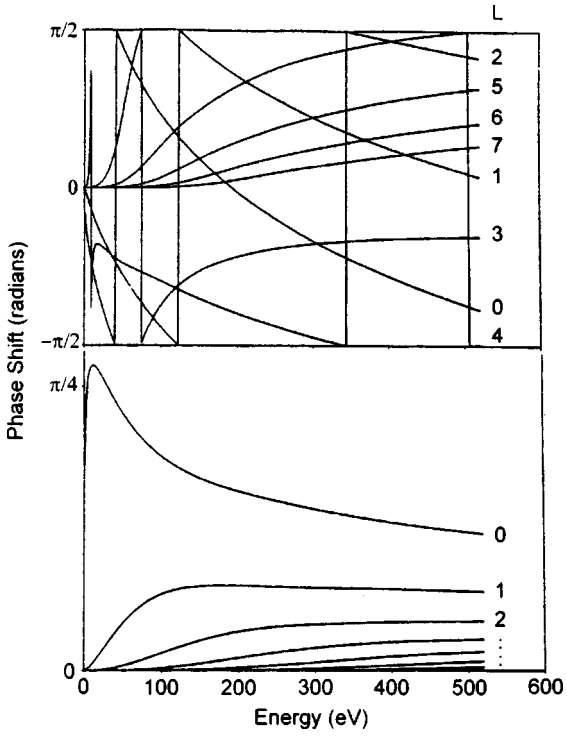

FIG. 3. Phase shifts used in the LEED intensity analysis for Rh (upper panel) and H (lower panel). The Rh phase shifts were constructed by overlapping nonrelativistic atomic potentials in the bulk Rh lattice leading to $r_{\text{mt}}=1.34$ Å and $V_{\text{mt}}=-19.6$ eV. The H phase shifts were obtained by superposing atomic potentials in a simple cube of side 1.337 Å taken to be twice the radius obtained by subtracting the bulk Rh radius from the H-Rh distance in the calculated fourfold adsorption site on Rh(001). The resulting muffin tin potential is $V_{\text{mt}}=-13.4$ eV.

IV. STRUCTURE ANALYSIS

Structure searches were based on comparing calculated intensities with experimental data using r factors proposed by Van Hove and Tong[17] (r_{VHT}), Zanazzi and Jona[26] (r_{ZJ}),

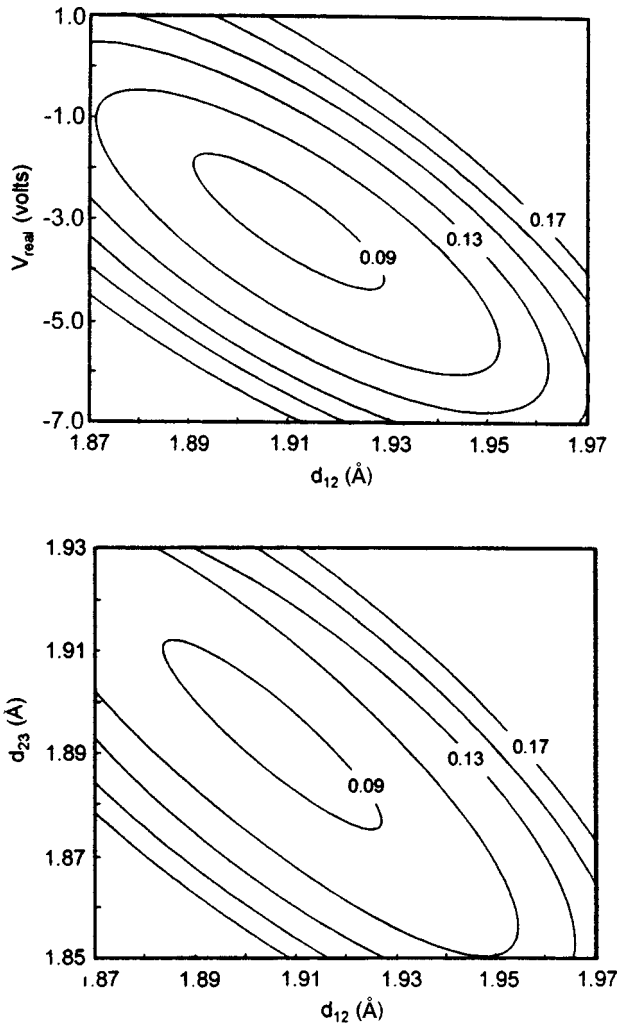

FIG. 4. Typical Zanazzi-Jona r factor contour plots showing variation of r factor with d_{12} and d_{23} and d_{12} and V_0.

Pendry[27] (r_P), and Duke *et al.*[28] (r_2'). Two independentanalyses were performed on all three sets of clean Rh(100) intensity data. Using the Van Hove/Tong codes, we performed a conventional structure search based on examining r factor contour plots as functions of structural and nonstructural parameters to minimize each of the three r factors as functions of V_0, V_{0i}, d_{12} and d_{23}. V_0, the real part of the inner potential, was taken as an adjustable parameter used to fit the measured LEED intensities.[28] The d_{ij} are the interlayer spacings between layers i and j. In a typical first pass search we varied d_{23} from 1.84–1.92 Å while allowing d_{12} to vary from 1.85–2.05 Å—both by 0.02 Å steps. In each case, the inner potential was varied by ±2 eV in 1 eV steps (around -3.0 eV) and all three r factors were calculated. A second pass was performed using a mesh of 0.01 Å for d_{12} and d_{23}, and repeated calculations were carried out in the vicinity of the minimum to verify the parameters. In Fig. 2 we display the calculated intensity profiles which minimize the Zanazzi-Jona r factor for clean Rh(001) superimposed on experimental data. Best fits were obtained with $V_0=-3$ eV, $V_{0i}=-6$ eV, and no $E^{1/3}$ or $E^{1/2}$ dependence. Selected contour plots that characterize the r factor convergence are shown in Fig. 4 also for the Zanazzi-Jona r factor. The results of these analyses are presented in Table II.

Independently we performed a structure analysis using the automated software described by Duke *et al.*[28] as applied previously, e.g., to PbTe(100).[29] This software uses the r_2' r factor as the fitting figure of merit in order that the curvature of the r factor at its minimum describes the uncertainties associated with those in the experimental measurement. A complete description of the use of this software is given by Lazarides *et al.*[29] The structural parameters are given in Table III. A comparison of the measured and calculated intensities is shown in Fig. 5.

This analysis establishes two important results. First, completely consistent results are obtained using graphical techniques and conventional r factors as well as using automated search techniques and the statistically significant r factor[28] r_2'. Second, using r_2' we get an estimate of the uncertainties in the structural parameters due to those in the experimental data alone. These are, as expected,[29] much smaller than those obtained using multiple r factors and incorporating the influence of uncertainties in the model as well. They are given in Table IV.

Calculations for the hydrogen-terminated surface were initially carried out with the same Van Hove/Tong LEED code set up for analyzing the clean Rh(001) surface. We adopted this approach because of the weak scattering intensity from H. The code was then modified to include scattering contributions from H atoms in the fourfold hollow sites, which correspond to the calculated[23,30] lowest total energy binding sites. When applied to the H covered Rh(001) data sets, both models yielded the same (within ±0.01 Å) H modified values for d_{12} and d_{23} presented in Table II: $d_{12}'=1.98\pm0.02$ and $d_{23}'=1.86\pm0.01$. The more sophisticated model also permitted evaluation of the H-Rh(001) interpla-

TABLE III. Results of a simplex structure search using the Xerox matrix-inversion code followed by a quadratic fitting procedure on three experimental data sets for the Rh(001) surface. The r factor r_2' as defined in Ref. 28 was used as the goodness of fit criterion. The remaining interlayer spacings have the bulk value of 1.902 Å and V_{0i} is 4.00 eV in each case. r_x is the x-ray r factor defined in Ref. 26.

Data set	Structure	d_{12} (Å)	d_{23} (Å)	V_0 (eV)	r_2'	r_x
RT1	Unrelaxed	1.902	1.902	3.250	0.056	0.069
	Best fit	1.910	1.897	2.995	0.055	0.068
RT2	Unrelaxed	1.902	1.902	3.250	0.107	0.091
	Best fit	1.932	1.885	3.435	0.092	0.081
LT3	Unrelaxed	1.902	1.902	3.250	0.065	0.051
	Best fit	1.927	1.878	3.025	0.052	0.046

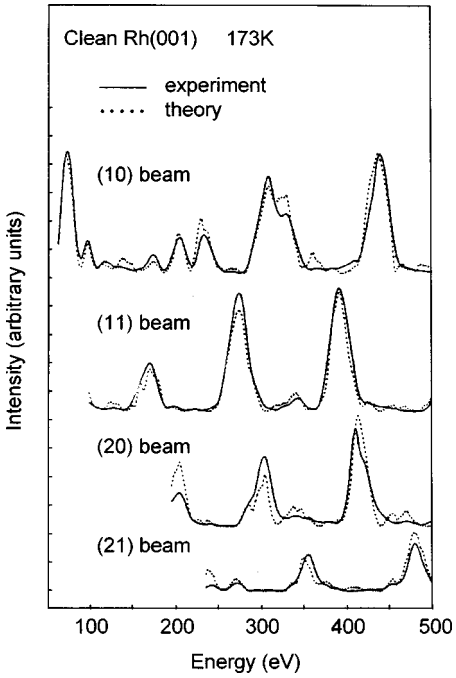

FIG. 5. Measured and calculated LEED intensity profiles obtained using the Xerox matrix-inversion codes and the r_2' r factor to determine the Rh(001) surface structure using the data set RT1.

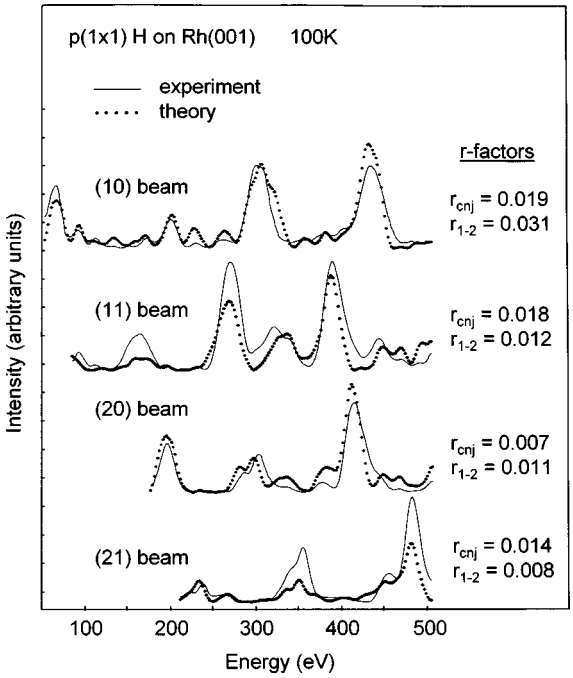

FIG. 6. Measured and calculated LEED intensity profiles from the Van Hove/Tong codes for $p(1\times1)$H on Rh(001). The H atoms are located at the four fold hollow sites on the Rh(001) surface. The r factors characterize agreement between theory and experiment.

nar distance. A structure search based on variation of the H-Rh(001) interplanar distance from 0.80 to 1.00 Å in 0.02 Å steps yielded $d_H = 0.88 \pm 0.5$ Å. Visual inspection was used to verify that the r factor minimization process yielded, in all cases, calculated curves in agreement with experimental data as shown in Fig. 6. Visual inspection and r factors indicate that the structure search for $p(1\times1)$ H on Rh(001) yielded less favorable agreement between theoretical and experimental LEED intensities compared to the clean Rh(001) results.

Our analysis of both the clean and H saturated Rh(001) surface considered only first (d_{12}) and second (d_{23}) layer relaxation, and did not consider any lateral displacements. The excellent agreement between experimental and theoretical results for clean Rh(001) and the very small changes in d_{12} and d_{23} from bulk values justifies the assumption that d_{34} and higher interplanar spacings remain equal to bulk lattice values. However, the much larger changes for d_{12} and d_{23} for the $p(1\times1)$ H on Rh(001) (refer to Fig. 7) suggest that corresponding changes of d_{34} and perhaps d_{45} should be included in the parameter search to refine the structure analysis. In order to determine if departure of d_{34} from the bulk value is responsible for the less favorable r factors in structure searches for the H saturated Rh(001) surface the structure model was extended to allow variation of d_{34}. An ex-

TABLE IV. Intrinsic structural uncertainties due to those in the measurements alone for the optimal structures obtained by minimizing r_2'. These are obtained as described by Lazarides *et al.* (Ref. 29). The d_{ij} are measured in Å. V_0 is measured in eV.

	Data set		
Parameter	RT1	RT2	LT3
d_{12}	0.001	0.001	0.001
d_{23}	0.001	0.002	0.001
V_0	0.009	0.019	0.014

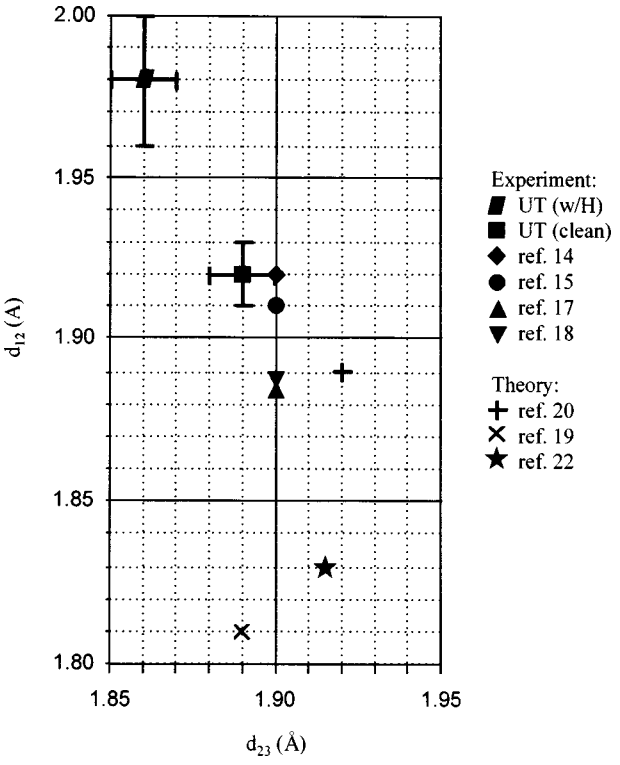

FIG. 7. Summary of various experimental and theoretical values of $\Delta d_{12}/d_0$ and $\Delta d_{23}/d_0$ for Rh(001).

tensive structure search in which d_{12}, d_{23}, and d_{34} were varied yielded the best r factors when $d_{34}=d_{\text{bulk}}$, and with the same values for the H-Rh(001) interplanar distance d'_{12} and d'_{23} given in the table. The results of all five structure searches are compiled in Table II, and the results for d_{12} and d_{23} are plotted in Fig. 7 along with previous experimental and theoretical values.

V. DISCUSSION

The picture of the structure of clean Rh(001) that emerges from our analysis is that the second layer relaxes inward toward the substrate by about 0.01 Å and its spacing from the surface layer increases commensurately (or perhaps a little more) leaving the surface layer unrelaxed (or perhaps slightly expanded) relative to the substrate. The effect is very small: its predicted magnitude depends both on the data set and on the r factor used as the optimization criterion. The Pendry r factor consistently gives larger changes in the layer spacings than any of the other three r factors. If we were to use the statistically meaningful r'_2 factor alone, we would obtain

$$d_{12}=1.921\pm0.011\ \text{Å} \quad \text{or} \quad \Delta d_{12}/d_0=+1.0\%\pm0.6\%$$

$$d_{23}=1.888\pm0.010\ \text{Å} \quad \Delta d_{23}/d_0=-0.7\%\pm0.5\%$$

for consistency between all three data sets, indicating that a slightly (by 0.01 Å) expanded top layer relative to the substrate (i.e., expanded by 0.02 Å relative to the second layer that is contracted by 0.01 Å relative to the substrate) is just barely outside the uncertainties associated with the data alone. This structure leads to intensity profiles which are visually indistinguishable from those of the unrelaxed surface. Thus, for practical purposes, the LEED intensity analysis yields an unrelaxed clean Rh(100) surface to within the uncertainties inherent in the analysis.[28,29]

The adsorption of a monolayer of hydrogen changes the LEED spectra and structure of Rh(001) significantly (see, e.g., Fig. 8). The LEED intensity analysis reveals that hydrogen adsorption enhances both the outward relaxation of the surface layer and the inward relaxation of the layer beneath, both to the extent that they lie outside the experimental 68% confidence limits for the clean surface.

A few comments about the prior LEED work for Rh(001) seem in order since early work[6,7] suggests d_{12} is slightly expanded, while more recent results[8,9] suggest a significant contraction. We digitized published IV spectra of Begley *et al.*[8] and Oed *et al.*[7] and compared them with our data. Based on the sensitivity of LEED intensity of the (01) beam around 350 eV to H and C surface contamination (displayed in Fig. 8) we believe that all of the data were obtained on essentially clean surfaces. Comparing the data sets based on r factor analysis shows (unsurprisingly) that the data of Oed *et al.*[7] are more compatible with our data sets: r_{zj} ranged from 0.04 to 0.06 and r_x ranged from 0.02 to 0.05 both yielding minimas at the same value of energy offset. These are very low r factors, which indicate an excellent match between the independent data sets measured by different experimental groups. (Compare with Fig. 2 and Table II.) Corresponding r factors comparing the data of Begley *et al.*[8] data with ours are larger: $r_{zj}=0.30-0.150$ and $r_x=0.040-0.114$.

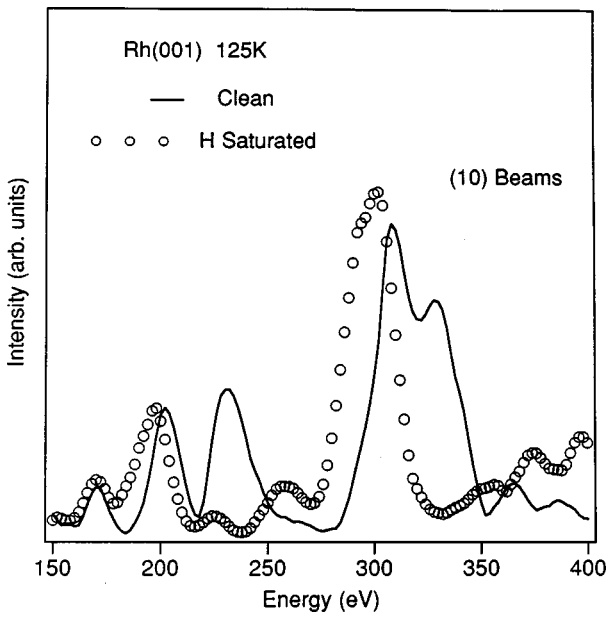

FIG. 8. Sensitivity of the intensity of the (10) beams to the presence of surface hydrogen.

Begley *et al.*[8] place generous error bars on their structural parameters, possibly justified by the apparent difficulty of obtaining highly consistent results from their data sets based on one of the r factors they employed (the Zanazzi-Jona r factor). We were able to obtain consistent results with acceptably low r factors using all three traditional r factors, as well as the statistically significant r'_2 criterion.

In summary, we have shown that the surface layer of clean Rh(001) exhibits a small outward relaxation relative to the second layer ($\Delta d_{12}=+1.0\%\pm0.6\%$), and that chemisorbed H significantly increases the relaxation ($\Delta d_{12}=+3.6\%\pm1.0\%$) as expected. Our measured H-Rh(001) interplanar distance $d_{\text{Rh-H}}=0.88\pm0.05$ Å is significantly larger than the calculated value (0.66 Å) obtained by Feibelman.[30] While visual comparison of our clean surface Rh(001) data with that of Oed *et al.*[7] and Begley *et al.*[8] based on results displayed in Fig. 8 suggests that all of the experimental data were obtained on essentially clean surfaces, the close agreement between our data and that of Oed *et al.*[7] and the broader energy ranges of these LEED studies suggest that an essentially unrelaxed surface structure for clean Rh(001) with perhaps a very small (0.01 Å) net outward relaxation of the surface layer relative to the substrate is the consensus result of the LEED intensity analyses. Thus, a clearly documented and unresolved discrepancy exists between state-of-the-art *ab initio* predictions of the Rh(001) structure and its experimental description by LEED intensity analyses.

ACKNOWLEDGMENTS

This work was supported by the R. A. Welch Foundation and by NSF DMR Grant No. 9623494.

[1] P. J. Feibelman and D. R. Hamann, Surf. Sci. **234**, 377 (1990).
[2] P. J. Feibelman, Surf. Sci. **360**, 297 (1996).
[3] I. Morrison, D. M. Bylander, and L. Kleinman, Phys. Rev. Lett. **71**, 1083 (1993).
[4] A. Eichler, J. Hafner, J. Furthmuller, and G. Kresse, Surf. Sci. **346**, 300 (1996).
[5] J.-H. Cho and M. Scheffler, Phys. Rev. Lett. **78**, 1299 (1997).
[6] P. R. Watson, F. R. Shephard, D. C. Frost, and K. A. R. Mitchell, Surf. Sci. **72**, 562 (1978).
[7] W. Oed, B. Dotsch, L. Hammer, K. Heinz, and K. Muller, Surf. Sci. **207**, 55 (1988).
[8] A. M. Begley, K. S. Kim, F. Jona, and P. M. Marcus, Phys. Rev. B **48**, 12 326 (1993).
[9] K. C. Prince, B. Ressel, C. Astaldi, M. Peloi, R. Rosei, M. Polcik, C. Crotti, M. Zacchigua, C. Comicioli, C. Ottaviani, C. Quaresima, and P. Perfetti, Surf. Sci. **377**, 117 (1997).
[10] H. L. Davis, J. B. Hannon, K. B. Ray, and E. W. Plummer, Phys. Rev. Lett. **68**, 2632 (1992); P. J. Sprunger, K. Pohl, H. L. Davis, and E. W. Plummer, Surf. Sci. **297**, L48 (1993).
[11] M. Methfessel, D. Hennig, and M. Scheffler, Phys. Rev. B **46**, 4816 (1992).
[12] R. Smoluchowski, Phys. Rev. **60**, 661 (1941).
[13] M. W. Finnis, and V. Heine, J. Phys. F **4**, L37 (1974).
[14] P. J. Feibelman, Phys. Rev. B **46**, 2532 (1992).
[15] S. C. Wu, K. Garrison, A. M. Begley, F. Jona, and P. D. Johnson, Phys. Rev. B **49**, 14 081 (1994).
[16] L. J. Richter, T. A. Germer, J. P. Sethna, and W. Ho, Phys. Rev. B **38**, 10 403 (1988).
[17] M. A. Van Hove and S. Y. Tong, *Surface-Crystallography by LEED* (Springer, Berlin, 1979).
[18] R. J. Meyer, C. B. Duke, A. Paton, A. Kahn, E. S., J. L. Yeh, and P. Mark, Phys. Rev. B **19**, 5194 (1979).
[19] W. K. Ford, T. Guo, D. L. Lessor, and C. B. Duke, Phys. Rev. B **42**, 8952 (1990).
[20] F. Herman and S. Skillman, *Atomic Structure Calculations* (Prentice-Hall, Englewood Cliffs, NJ, 1963).
[21] J. C. Slater, Phys. Rev. **81**, 385 (1951).
[22] D. W. Jepsen, P. M. Marcus, and F. Jona, Phys. Rev. B **5**, 3933 (1972).
[23] P. J. Feibelman, Phys. Rev. Lett. **67**, 461 (1991).
[24] C. B. Duke, A. Paton, W. K. Ford, A. Kahn, and J. Carelli, Phys. Rev. B **24**, 562 (1981).
[25] *American Institute of Physics Handbook*, edited by D. E. Gray, 3rd ed. (McGraw-Hill, New York, 1972), pp. 4–116.
[26] E. Zanazzi and F. Jona, Surf. Sci. **62**, 61 (1977).
[27] J. B. Pendry, J. Phys. C **13**, 937 (1980).
[28] C. B. Duke, A. A. Lazarides, A. Paton, and Y. R. Wang, Phys. Rev. B **52**, 14 878 (1995).
[29] A. A. Lazarides, C. B. Duke, A. Paton, and A. Kahn, Phys. Rev. B **52**, 14 895 (1995).
[30] P. J. Feibelman, Phys. Rev. B **43**, 9452 (1991).